PHYSICAL REVIEW B VOLUME 16, NUMBER 10 15 NOVEMBER 1977

Multiple-trapping model of anomalous transit-time dispersion in a-Se

J. Noolandi
Xerox Research Center of Canada, 2480 Dunwin Drive, Mississauga, Ontario L5L 1J9, Canada
(Received 17 December 1976; revised manuscript received 29 July 1977)

A generalized model of multiple trapping from a band of extended or localized states is used to study time-dependent charge transport in amorphous solids. The model differs from a conventional multiple-trapping model by including a distribution of trap release rates for a constant trap energy. An extensive analysis of transient photocurrent experiments on a-Se is carried out to determine the transport parameters for this case. It is found that a small number of parameters can be used to analyze the experimental results over a wide range of temperature and sample thickness. The results of the analysis are interpreted in terms of trap-controlled hopping, which is a special case of the generalized multiple-trapping model. The asymptotic value of the theoretical photocurrent transient is obtained for the multiple-trapping model, and the results of Scher and Montroll are recovered for the case of extreme or anomalous dispersion, which occurs for a-Se at low temperature ($T \simeq 140$ K). The density of trapping sites is estimated, and the difficulties associated with considering a continuous distribution of trap release rates are discussed. It is concluded that the generalized multiple-trapping model, defined by simple first-order rate equations, is capable of describing detailed shapes of photocurrent transients, including dispersive and nondispersive charge transport.

I. INTRODUCTION

Considerable information on the physics of charge transport in amorphous materials has been developed[1-3] and recently stimulated by the work of Pfister,[2] using the time-of-flight technique to study photoinduced transient conductivity in chalcogenide glasses and other materials. In particular the large body of experimental data on a-As_2Se_3 verified the predictions of the Scher-Montroll (SM) theory[4] of anomalous dispersion of the observed photocurrent transients. SM developed a model which describes the dynamics of charge carriers executing a time-dependent random walk on a simple cubic lattice, under the influence of an external electric field. The SM model starts from a generalized non-Markoffian master equation to describe the transport process, and requires mathematical analysis of considerable complexity to obtain asymptotic solutions for the photocurrent transients. In this paper it is shown that a wide range of dispersion in photocurrent transients can be understood using a generalized multiple-trapping model. In the following paper[5] (hereafter referred to as II) it is shown that the first-order linear rate equations describing multiple trapping are formally equivalent to the continuum limit of the SM master equation.

Since the multiple-trapping model is formally equivalent to the continuous-time-random-walk (CTRW) model of SM, it is not surprising that different classes of charge transport can all be described by the multiple-trapping theory. Conventially, the distribution of release rates from traps, $r_i = \alpha_i \exp(-E_i/k_BT)$, arises from variations in the activation energy. In the generalized model both the prefactor α_i and the activation energy E_i may vary and contribute to a distribution of the r_i. A continuous distribution of r_i for constant E_i, may be conveniently described as "hopping"; however, the classification of different models of charge transport is largely a matter of taste, since they can all be described as special cases of a more general model.

In the absence of information about the trap density of states, we assume for the a-Se analysis that the distributions of trapping parameters may be approximated by a small number of discrete levels. This assumption is justified by the successful description, in terms of a consistent set of parameters, of photocurrent transient shapes over a wide range of temperature and sample thickness. In II these parameters are used to compute the SM waiting-time distribution function $\psi(t)$ for different temperatures. Agreement with the power-law behavior of $\psi(t)$, assumed by SM, is obtained for low temperature ($T \sim 140$ K) and the evolution of $\psi(t)$ to an exponential characteristic of nondispersive transport is found for higher temperature ($T \sim 250$ K).

Although the idea of conventional multiple trapping has been discussed by a number of workers previously,[3] the first analytic solution of the problem has been given recently by Schmidlin[6] and Rudenko.[7] In the present paper the generalized multiple-trapping model is developed to determine the conditions for obtaining very disperse photocurrent transients. In addition, a large amount of experimental data on a-Se is analyzed, and specific values for the transport parameters as a function of temperature are obtained for a model with three effective trap levels. The distribution

of release rates from the trap levels is found to originate from variations in the prefactor, rather than the activation energy, and the change in dispersion with temperature is accounted for by the temperature dependence of the capture rates.

In Sec. II the multiple-trapping model is formulated, and the expression for the Laplace transform of the photocurrent transient for a strongly absorbed light flash is derived. The results of the analysis of the experimental data for a-Se are given in Sec. III, where the superlinear behavior of the apparent transit time on sample length is calculated and compared to experiment. The asymptotic behavior of the theoretical photocurrent transient for the multiple-trapping model is obtained in Sec. IV, and shown to be identical to the asymptotic behavior in the SM model. We show that just three types of traps with release rates distributed uniformly on a logarithmic scale give rise to the anomalous dispersion discussed by SM. We also discuss the case of a continuous distribution of trap states, the concentration of trap states, and the interpretation of the results in terms of trap-controlled hopping. The results are summarized in Sec. V.

II. MULTIPLE-TRAPPING MODEL

The multiple-trapping model for unipolar conduction is defined by the following equations[6,7]:

$$\frac{\partial \rho(\vec{x}, t)}{\partial t} = g(\vec{x}, t) - \vec{\nabla} \cdot \vec{f}(\vec{x}, t), \tag{1}$$

where

$$\rho(\vec{x}, t) = p(\vec{x}, t) + \sum_i p_i(\vec{x}, t) \tag{2}$$

and

$$\frac{\partial p_i(\vec{x}, t)}{\partial t} = p(\vec{x}, t)\omega_i - p_i(\vec{x}, t)r_i . \tag{3}$$

As discussed in the following paper[5] this model is a simple special case of a more general model formulated in terms of linear transport equations.[8] Here $\vec{x} \equiv (x_1, x_2, x_3)$, t is time, and we consider a photoconductor of finite thickness, $0 \le x_1 \le L$, but otherwise infinite in extent. The local photogeneration rate is denoted by $g(\vec{x}, t)$, and $\vec{f}$ is the flux of mobile charge carriers. The total concentration of carriers is $\rho(\vec{x}, t)$, defined by Eq. (2). The summation in Eq. (2) extends over all the different kinds of traps in the material. Each trap is characterized by a capture rate ω_i and a release rate r_i. The trap parameters are assumed to be independent of position, corresponding to a homogeneous trap distribution. The concentration of mobile carriers is $p(\vec{x}, t)$, and $p_i(\vec{x}, t)$ is the concentration of carriers temporarily immobilized in the ith trap.

In order to solve Eqs. (1)–(3) it is necessary to specify the initial concentrations of mobile and trapped carriers $p(\vec{x}, 0)$ and $p_i(\vec{x}, 0)$, respectively, and to relate the flux of mobile carriers to the carrier concentration. For a broad range of conditions, it is possible to neglect diffusion, allowing us to write

$$\vec{f} = \vec{v}p \tag{4}$$

and

$$\vec{v} = \mu_0 \vec{E}, \tag{5}$$

where μ_0 is the mobility of the free carriers. In writing Eq. (5) we have assumed that it is possible to characterize the velocity of the mobile carriers by a field-independent mobility. In general it is also necessary to supplement Eqs. (1)–(3) by Poisson's equation in order to determine $\vec{E}(\vec{x}, t)$. In the present problem however we restrict ourselves to the discussion of small photocurrent signals, with a constant voltage maintained across the sample, and we consider the electric field as constant.

For a strongly absorbed light flash the local photogeneration rate can be written

$$g(\vec{x}, t) = \eta \delta(\vec{x}) \delta(t), \tag{6}$$

where η is the photogeneration efficiency, and we assume $p(\vec{x}, 0) = p_i(\vec{x}, 0) = 0$. Using Eqs. (4)–(6), Eqs. (1)–(3) can be solved using the Laplace-transform (LT) technique for first-order rate equations.[6,9] Defining

$$\tilde{p}(\vec{x}, s) = \int_0^\infty e^{-st} p(\vec{x}, t)\, dt, \tag{7}$$

one obtains[6]

$$\tilde{p}(x, s) = (\eta/\mu_0 E) \exp[-a(s) t_0 x/L], \tag{8}$$

where $t_0 = L/\mu_0 E$ is the transit time of untrapped carriers, the electric field is in the x direction, and

$$a(s) t_0 = s\left(t_0 + \sum_i \frac{M_i}{s + r_i}\right), \tag{9}$$

where $M_i = \omega_i t_0$ is the number of times a carrier is captured by trap i alone while crossing the sample. The measured current $I(t)$ is given in terms of the spatial average of the flux of free carriers across the sample, hence

$$\tilde{I}(s) = \frac{e\mu_0 E}{L} \int_0^L \tilde{p}(x, s)\, dx, \tag{10}$$

where e is the charge of a carrier. Using Eq. (8), Eq. (10) gives

$$\tilde{I}(s) = (e\eta/t_0)\{[1 - \exp[-a(s)t_0]\}/a(s), \qquad (11)$$

which is the basic result for the transform of the photocurrent. Equation (11) is of the same form as Eq. (54) of SM.[4] This indicates there is a close connection between the multiple-trapping model and the SM model. This connection will be discussed in Sec. IV A of this paper, and in II. Here it should be noted that the mathematical analysis required to obtain Eq. (11) is elementary, and the effect of the absorbing boundary is included in a simple way by carrying out the integration in Eq. (10) between finite limits corresponding to the sample length.

The inverse of the current transform can be evaluated using the inverse LT tables.[10] The resulting expression involves a convolution of the modified Bessel function of first order and must, in general, be evaluated numerically. In the present analysis, it was convenient to evaluate the inverse of $\tilde{I}(s)$ numerically by deforming the contour of integration to a circle which encloses all the essential singularities along the negative real axis. The integration technique is described in Appendix A, and is more powerful than an earlier technique which was found to be effective only for very disperse transients.[11]

III. RESULTS OF a-Se ANALYSIS

Experimental photocurrent transients for a-Se were analyzed for a range of temperatures (T = 122–293 K), electric fields (E = 2.5–10 V/μm), and sample thicknesses (L = 20–79 μm). A least-squares fit to each individual transient was carried out using Eq. (11) and the numerical LT inversion described in the Appendix. The number of capture events by each type of trap $M_i = \omega_i t_0$, the corresponding release rates r_i, and the amplitude of the photocurrent were treated as independent parameters for each transient. Each experimental curve was digitized and represented by about 50 points. Typical fits for low (T = 143 K), medium (T = 188 K), and high (T = 250 K) temperatures with E = 10 V/μm and L = 79 μm are shown in Figs. 1 and 2. Fits were carried out using different numbers of traps, and it was found that three different types of traps were sufficient to fit the data within a relative error of 5%. Using a large number of traps did not significantly improve the fits; moreover the parameters for additional traps fell within the spectrum of values already determined from the three-trap fit. In Fig. 1 the theoretical photocurrent transient shows small oscillations which are not present in the experimental curve. These oscillations occur because we are using a small number of discrete traps, and they disappear completely when a small amount of dispersion in the trap release rates is included in the model. In the present analysis these oscillations do not give rise to any difficulties, because they are small and can be ignored. From Figs. 1 and 2 the distinguishing feature of the photocurrent transients in a-Se, namely, the disappearance of dispersion with increasing temperature, can be seen clearly.

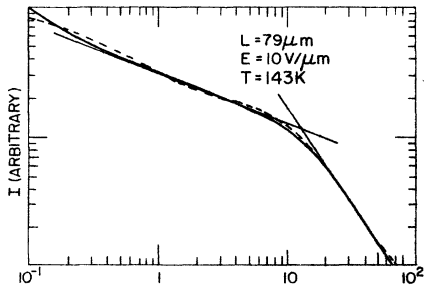

FIG. 1. Photocurrent transient for a-Se for the experimental conditions indicated. The solid line shows the experimental curve, and the two straight lines show pre-transit and post-transit slopes, which correspond to $-(1-\alpha)$ and $-(1+\alpha)$, respectively, according to the Scher-Montroll theory. The dashed line shows the best fit to experiment using the three-level multiple-trapping model.

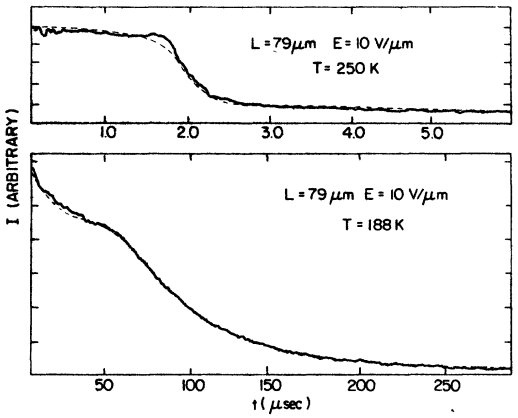

FIG. 2. Photocurrent transients for a-Se, showing a nondisperse transient for T = 250 K (upper panel) and a transient of "intermediate" dispersion for T = 188 K (lower panel). The dashed lines show the best fits to experimental data using the three-level multiple-trapping model.

The results of the three-trap fit for E = 10 V/μm and L = 79 μm are shown in Fig. 3. The photocurrent amplitude Q is not shown because absolute photocurrents were not measured and Q is merely a scaling factor. Although the number of physically relevant parameters is large (6), it should be noted that the fits were carried out independently for each temperature shown in Fig. 3, and the good correlation for different temperatures indicates that the parameters are meaningful.

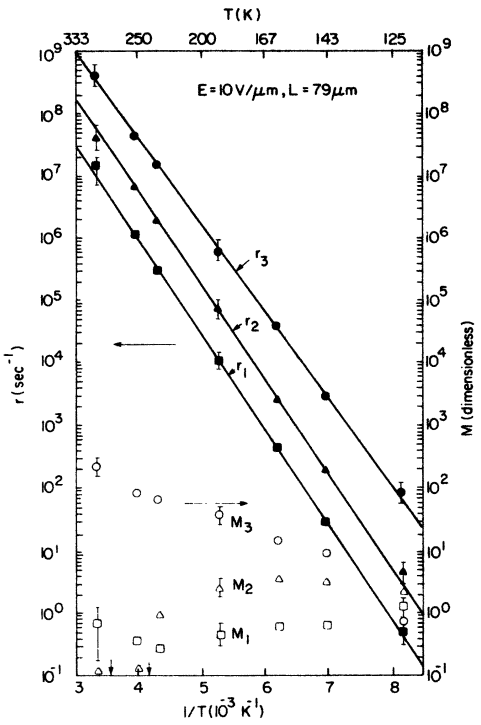

FIG. 3. Multiple-trapping parameters $r_i, M_i = \omega_i t_0$ for a-Se obtained by a least-squares fit of Eq. (11) to experimental data for each temperature indicated. The solid symbols indicate the release rates, and the open symbols indicate the corresponding number of trapping events.

Throughout the whole range of temperature the release rates for the three traps were found to have the same activation energy (~0.3 eV). Since $r_i = \alpha_i \exp(-\beta E_i)$ in general, the variation in the release rates at a given temperature arises solely from the variation in the prefactor, α_i. From Fig. 3 it can also be seen that the r_i are distributed uniformly on a logarithmic scale. The corresponding release times r_i^{-1} are distributed uniformly along the $\log_{10} t$ axis of the transient curve. For low temperatures ($T = 122$ K and $T = 143$ K) it was found that $M_i \sim 1$ for $r t_m \sim 1$, where the apparent transit time t_m is defined by the intersection of tangents to $I(t)$ for $t \ll t_m$ and $t \gg t_m$. For a discrete trap model, this means that maximum dispersion occurs when a charge carrier visits a trap with a long release time only once. Also, we found that

$$t_m \sim \sum_i{}' \frac{M_i}{r_i}, \tag{12}$$

where the prime indicates that only terms with $M_i \gtrsim 2$ are to be kept in the summation. Hence the apparent transit time is determined by the faster carriers which are trapped and released many times during transit.

Equation (12) is to be compared with the result

$$t_m = t_0\left(1 + \sum_i \frac{\omega_i}{r_i}\right), \tag{13}$$

which was obtained directly from the multiple-trapping equations using asymptotic methods, for $M_i \gg 1$, or $r_i t_m \gg 1$.[11] Equation (12) indicates that this result (with a restricted sum) gives a good approximation to t_m also in the general case. In the present numerical analysis the quantity t_0 by itself in Eq. (9) was neglected, because the free transit time can be estimated to be very small,[12] and is unobservable in Pfister's experiments.[2] For $T = 143$ K the approximate relation $M_i \propto r_i^{0.5}$ was found. The significance of this relation will be discussed in Sec. IV. For $T = 122$ K all the M_i were of order unity, and the approximate power-law relation was not as evident as for $T = 143$ K. A difficulty with the analysis for $T = 122$ K is that t_m is very long, and the tail of the photocurrent is difficult to observe for long times because the amplitude becomes very small.

As the temperature increases, the dispersion decreases; and at room temperature, photocurrent transients characteristic of nondispersive transport are observed. An interesting result of the analysis is that the disappearance of dispersion is accounted for solely by the temperature dependence of the M_i's. As the temperature increases, M_3 increases while M_1 and M_2 decrease. From Fig. 3, an activation energy of 0.06 eV can be estimated for M_3. The temperature dependence of the M_i reflects the fact that there is a sharpening in the shape of the transients with increasing temperature, while the observed activation energy for the mobility, defined by $\mu = L/t_m E$, remains constant.[2] Our analysis shows that the only way a constant activation energy for the mobility is consistent with a dramatic change in shape is to have a change in the M_i. This result was checked by introducing a shallow trap (activation energy ~0.1 eV) with a fixed large release rate greater than r_3 into the theoretical photocurrent expression. When the shallow trap was substituted for trap 3, the fit to experiment became poor, and when the shallow trap was included as a fourth trap in the three-trap fit, then $M_4 \sim 0$. Hence the disappearance of dispersion in a-Se cannot be attributed to the presence of shallow traps, or to the changing of deep traps into shallow traps as the temperature is increased.[13] At present there is no fundamental explanation for the temperature dependence of the M_i obtained here. However, it is hoped that the charge capture and release kinetics can be related to the properties of the low-lying defect states recently proposed for the chalcogenide glasses.[14,15] Finally, error bars typical of the un-

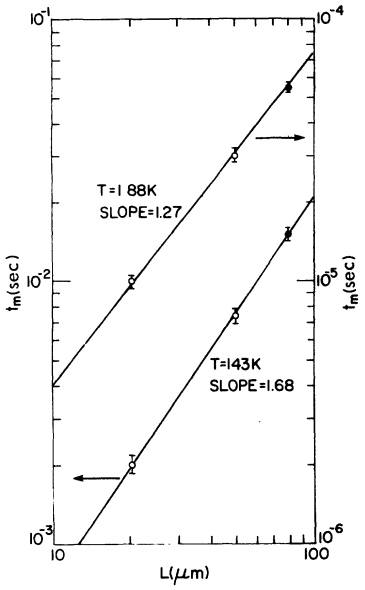

FIG. 4. Length dependence of apparent transit time t_m obtained from theoretically predicted photocurrent traces using the multiple-trapping parameters for a-Se with $E=10$ V/μm, $L=79$ μm, and the temperatures indicated. The solid circles correspond to experimental points, and the open circles denote predicted values.

certainty in the parameters have been included in Fig. 3. At room temperature relatively large errors are obtained for r_1 and r_2 because M_1 and M_2 are very small, and these traps have little effect on the shape of the transient.

The length dependence of t_m was investigated by scaling $M_i=\omega_i t_0=\omega_i L/\mu_0 E$ proportional to L. The trap parameters for the transients at $T=143$ K and $T=188$ K, with $L=79$ μm, were used to calculate the theoretical transients corresponding to $L=50$ μm and $L=20$ μm. The results for t_m are shown in Fig. 4, and exhibit the superlinear dependence on L observed experimentally.[2] At $T=143$ K the slopes of the experimental transient shown in Fig. 1 give $1-\alpha=0.42$ for $t<t_m$, and $1+\alpha=1.54$ for $t>t_m$. The sum of the slopes is 1.96, close to the theoretical value of 2 predicted by SM for very disperse transients.[4] According to the SM theory, the inverse of the slope in Fig. 4 is α^{-1}, giving $\alpha=0.59$ for $T=143$ K, in good agreement with the average value $\bar{\alpha}=0.56$ determined from Fig. 1. At higher temperatures the SM sum rule is no longer satisfied experimentally for a-Se, and the slopes of the $\log_{10}t_m$-vs-$\log_{10}L$ plots tend to unity. From Fig. 4 the value of the slope at $T=188$ K is 1.27, in good agreement with the experimental value of 1.34 obtained at $T=181$ K. The explanation of the superlinear behavior in terms of trapping events has been suggested earlier.[3] The sample thickness determines the number of times a trap is visited, and gives rise to a nonlinear thickness dependence for t_m. Analytically, the nonlinear dependence follows from Eq. (12) where the absolute value of M_i determines whether the corresponding trap should be included in the summation. Writing $t_m=L/\mu E$, the nonlinear dependence of t_m on L can be interpreted in terms of a thickness dependence of the mobility μ. However, this interpretation is misleading, since it is clear from the previous discussion that μ defined in terms of t_m is not an intensive quantity.

The analysis was also carried out for transients taken at a constant temperature and subjected to a variable electric field (2.5–10 V/μm). However, it was found that the range of fields investigated experimentally was too small to obtain meaningful trends in the parameters $\omega_i(E)$ and $r_i(E)=\alpha_i(E)\exp[-\beta E_i(E)]$. In particular it was not possible to distinguish between the different possible physical models for r_i.[12] More extensive measurements would establish the limitations of "universality" of the transient current shapes with respect to E, and would enable the determination of the functional dependence of the trap parameters on E.

IV. DISCUSSION

A. Asymptotic form of $I(s)$

The asymptotic behavior of the current transform can be studied using Eqs. (9) and (11). Defining

$$\Sigma(s)=s\sum_i \frac{M_i}{s+r_i}, \tag{14}$$

Eq. (9) becomes

$$a(s)t_0=st_0+\Sigma(s). \tag{15}$$

From the analysis of the a-Se photocurrent transients at low temperature ($T=143$ K), discussed in Sec. III, we found that the trap release rates were uniformly spaced on a logarithmic scale, and that the (discrete) capture rates were related to the release rates according to a power law

$$M_i \propto r_i^{\alpha} \text{ (discrete levels)}, \tag{16}$$

where $\alpha\simeq 0.5$ for $T=143$ K. This relation was found for the three-trap model used in the a-Se analysis. It is remarkable fact that, for just three different traps, with the appropriate parameters, the quantity $\Sigma(s)$ behaves approximately like a power law

$$\Sigma(s)\simeq s^{\alpha} \tag{17}$$

over two decades in s space. This behavior is

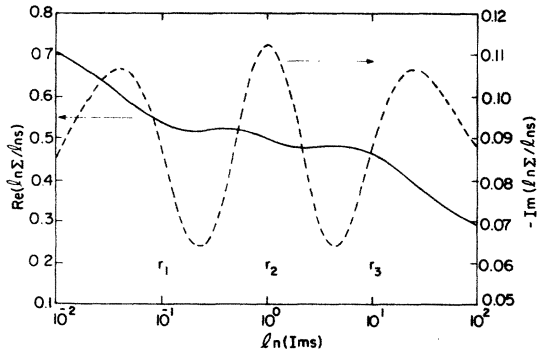

FIG. 5. Real and imaginary parts of $\ln\Sigma/\ln s$, with $\Sigma(s)$ defined by Eq. (14) and s along the imaginary axis. The plot shows the approximate power-law behavior of $\Sigma(s)$ using three traps, with r_i spaced uniformly along the logarithmic axis, and $\omega_i = r_i^{0.5}$.

shown in Fig. 5, where both the real and imaginary parts of $\ln\Sigma/\ln s$ have been calculated for s along the imaginary axis. For the purpose of this calculation, the proportionality constant in Eq. (16) was put equal to unity, and $\alpha = 0.5$. The variation in $\mathrm{Re}(\ln\Sigma/\ln s)$ was within ± 0.03 of 0.5 over the two decades in $\ln(\mathrm{Im}s)$ defined by the choice of the release states. The imaginary part of $\ln\Sigma/\ln s$ over the same range of $\ln(\mathrm{Im}s)$ was found to be small and oscillatory. Hence Eq. (15) may be approximated as

$$a(s)t_0 \simeq st_0 + cs^\alpha , \tag{18}$$

where c is a constant. For small s, with $0<\alpha<1$, the second term in Eq. (18) dominates the first. For very large s, $st_0 \gg cs^\alpha$. Since t_0 is estimated to be very small[12] however, the value of s such that $st_0 \gg cs^\alpha$ corresponds to extremely short times which are not easily accessible experimentally. Here we are not concerned with these short times and we ignore the first term in Eq. (18), so that

$$a(s)t_0 \propto s^\alpha . \tag{19}$$

Using Eq. (11) we then obtain the result

$$\tilde{I}(s) \propto \begin{cases} s^{-\alpha}, & a(s)t_0 \gg 1 , \\ s^\alpha, & a(s)t_0 \ll 1 , \end{cases} \tag{20}$$

which is the same result obtained by SM from solving the absorbing boundary problem. In the SM formalism,[4] the effect of the absorbing boundary is to cause a "time-dependent" transition in the branch point ($s^{-\alpha} \rightarrow s^\alpha$) in the Laplace transform of $I(t)$. In the multiple-trap formalism the same result is obtained from the power-law behavior of $\Sigma(s)$ for very disperse photocurrent transients, and the form of the current transform, Eq. (11).

B. Continuum distribution of trap states

Without any loss in generality one can write Eq. (14) as

$$\Sigma(s) = s\int_0^\infty \frac{M(r)g(r)}{s+r}\,dr , \tag{21}$$

where

$$M(r)g(r) = \sum_{i=1}^{n} M_i(r)\delta(r - r_i) , \tag{22}$$

and $g(r)$ is the density of states. From the results of the a-Se analysis it is tempting to assume

$$M(r)g(r)dr \propto r^\alpha d\ln r , \tag{23}$$

since Eq. (21) then becomes a Stieltjes transform,[10] which gives $\Sigma(s) \propto s^\alpha$. We would like to point out that there is not enough information in the shapes of the photocurrent transients to uniquely determine the functional form of *both* $M(r)$ and the density of states, $g(r)$. As an example of this indeterminacy, as we have just seen, a three-level discrete trap model also gives a power-law dependence of $\Sigma(s)$. Hence it is not clear whether the relation $M(r) \propto r^\alpha$ has any significance in the continuum limit, since other choices for the functional form of $M(r)$, along with the density of states $g(r)$ can also give a power-law dependence of $\Sigma(s)$. In order to uniquely determine $M(r)$ the density of trap states should first be determined independently from other experiments on the same samples.

C. Concentration of trap states

Having determined the trap parameters $\{\omega_i, r_i\}$ from the a-Se analysis, we now use the principle of detailed balancing to provide a connection between ω_i and r_i, thereby determining the concentration of trap states N_i. We write

$$\omega_i = N_i a_i , \quad r_i = \alpha_i \exp(-\beta E_i) , \tag{24}$$

where N_i is the concentration per unit volume of trap i. The steady-state solution of Eq. (3) gives

$$\frac{p_i}{p} = \frac{\omega_i}{r_i} = \frac{N_i a_i}{\alpha_i \exp(-\beta E_i)} , \tag{25}$$

whence $a_i = \alpha_i / N_v$ from the principle of detailed balancing, and N_v is the concentration per unit volume of valence states. Hence

$$N_i/N_v = \omega_i/\alpha_i = M_i/\alpha_i t_0 , \tag{26}$$

where M_i is the number of times a carrier is captured by trap i alone while crossing the sample, and $t_0 = L/\mu_0 E$ is the transit time of free carriers. Assuming a microscopic hole mobility $\mu_0 \propto T^{-3/2}$, and using the value $\mu_0 = 0.34 \pm 0.005$ $\mathrm{cm}^2/\mathrm{V\,sec}$ at room temperature,[12] t_0 can be calcu-

lated for a given sample thickness L, electric field E, and temperature T. From Fig. 3, the slowest trap in a-Se for maximum dispersion at $T = 143$ K has the parameters $M_i \sim 1$, $\alpha_i \sim 10^{12}$ sec^{-1}, and using Eq. (26) with $L = 75$ μm, $E = 10$ V/μm gives $N_i/N_v \sim 10^{-5}$, which agrees with corresponding values determined elsewhere.[12] Assuming a concentration of states at the valence-band edge of $N_v \sim 10^{20}$ cm^{-3},[12] gives $N_i \sim 10^{15}$ cm^{-3}, in agreement with accepted values of $N_i \sim 10^{15}$–10^{17} cm^{-3}.[12]

D. Interpretation in terms of trap-controlled hopping

From Fig. 3, it is seen that the prefactors of the release rates vary by two orders of magnitude. For the case of trap-controlled hopping one can write[13]

$$\alpha_i = W_0 \exp(-R_i/R_0), \tag{27}$$

where W_0 is a transition rate, and R_0 is the radius of the local charge distribution. Assuming $W_0 \sim 10^{20}$ sec^{-1} (Ref. 13) gives R_i/R_0 in the range 10–20 for α_i in the range 10^{12}–10^{14}, in agreement with values obtained for other amorphous materials.[13] In the case of trap-controlled hopping the small number of trapping events refers only to hopping sites where the carrier encounters long hops. Thus, although there is a large number of hopping events, which corresponds to transport through a hopping "band" in the generalized multiple-trapping model, the anomalous dispersion arises entirely from the few trapping events where the carrier is held back for a long time. The concentration of trapping states obtained in Sec. IV C then refers to the hopping states which are relatively well separated from the remaining states by their long release times. Thus, unlike the conventional multiple-trapping model, the generalized model includes trap-controlled hopping as a special case.

V. CONCLUSIONS

In the multiple-trapping model, a small number of charge capture and release events from traps with release times on the order of the time scale of the experiment gives rise to the kind of anomalous or extreme dispersive transport discussed earlier by Scher and Montroll. Trapping takes place from a band of extended states or a band of localized states which are responsible for charge transport in the material. The small number of trapping events can be interpreted in terms of trap-controlled hopping, in which only hopping sites with long release times are called "traps." The apparent transit time t_m is given approximately by the amount of time carriers spend in traps with fast release times, and the predicted superlinear behavior of t_m on sample thickness L is in good agreement with the experiment.

The change in shape of the photocurrent transients in a-Se with temperature is explained solely by the temperature dependence of the trap capture events $M_i = \omega_i L/\mu_0 E$, and the activation energy of the release rates r_i is constant up to room temperature. It is a remarkable fact that only three effective trap levels are sufficient to describe the shapes of photocurrent transients over a wide range of dispersion. A detailed study of these shapes through the transition from dispersive to nondispersive transport shows no evidence for a deep trap changing to a shallow trap with increasing temperature.[13]

A study of the asymptotic value of the theoretical photocurrent transient for the multiple-trapping model shows how the Scher-Montroll results can be recovered at low temperature for a-Se. The general connection between the multiple-trapping model and continuous-time random walk is discussed in II.

A continuous spread in release times from traps can be described easily in the multiple-trapping model by using an integral representation of the sums over trap indices. However, in order to obtain information about the functional form of $\omega(r)$ by comparison with experimental photocurrent transients, it is necessary to obtain the trap density of states $g(r)$ independently. From the a-Se analysis there is no evidence that $\omega(r) \sim r^{\alpha}$ in the continuum limit of a trap distribution. The approximate power law relation is valid only for a *discrete* set of trap levels, with the trap release rates spaced uniformly on a logarithmic scale. However the concentration of trap states can be estimated for a-Se, giving $N_i = 10^{15}$ cm^{-3}.

The conventional multiple-trapping model can describe a distribution of $r_i = \alpha_i \exp(-E_i/k_B T)$ only by introducing a distribution of energy levels E_i. In the generalized model a distribution of prefactors α_i can also be important. Recent work[14,15] has shown that a large number of electronic defect states, having approximately the same energy levels, can exist in the chalcogenide glasses. It is the task of future work to understand the charge capture and release kinetics of the effective trapping levels introduced here in terms of the structural disorder of the material, and the properties of the valence-alternation pair states.[14,15]

In general it is concluded that the multiple-trapping model is easy to solve analytically and easily applied to an analysis of experimental data. The model can describe the detailed shapes of photocurrent transients, using a small number of parameters and can be used to analyze a wide range of dispersion in charge transport.

ACKNOWLEDGMENTS

We would like to thank G. Pfister for his photocurrent transient data on a-Se, and G. C. Hartmann for discussions and encouragement. We would also like to thank L. M. Marks for assistance with the mathematical and numerical analysis, and F. W. Schmidlin and H. Scher for discussions on the theory of multiple trapping.

APPENDIX

We describe the procedure used to numerically invert the Laplace transform of the transient photocurrent $\tilde{I}(s)$, where

$$\tilde{I}(s)=\{1-\exp[-a(s)t_0]\}/a(s) \tag{A1}$$

and

$$a(s)t_0=\sum_i \frac{sM_i}{s+r_i}\,. \tag{A2}$$

As discussed in Secs. III and IV, the term st_0 has been neglected in Eq. (A2). We first note that

$$\lim_{s\to\infty}\tilde{I}(s)=\left[1-\exp\left(-\sum_i M_i\right)\right]\Big/\sum_i M_i\,, \tag{A3}$$

and we subtract this term from $\tilde{I}(s)$ in order to eliminate the corresponding $\delta(t)$ singularity in $I(t)$. Next we see that $\tilde{I}(s)$ has essential singularities at $s=-r_1,\ldots,-r_1,\ldots,-r_N$, where there are N traps and $0\le r_i<\infty$.

A convenient contour for evaluating

$$L^{-1}(\tilde{I}(s))=\int_C \tilde{I}(s)e^{st}\,ds \tag{A4}$$

numerically is the circle shown in Fig. 6, where $|s-s_1|=R$ and $s_1=(-R_1,0)$. R and R_1 are chosen subject to the constraints

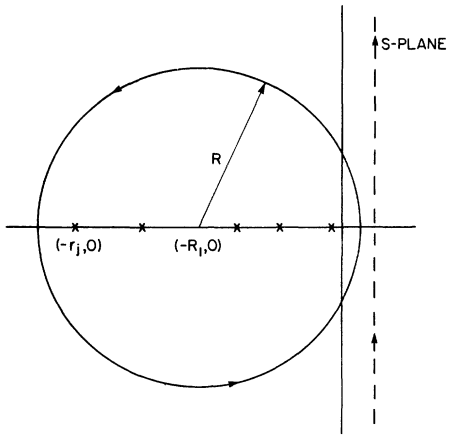

FIG. 6. Contour of integration in the complex s plane used for numerical evaluation of $I(t)$ (cf. Appendix). The crosses indicate the location of essential singularities in $\tilde{I}(s)$.

$$R-R_1=\epsilon,\quad R+R_1>\max(r_i)\,, \tag{A5}$$

where ϵ is a small positive number. It can then be shown that

$$|\exp[-a(s)]|<1 \tag{A6}$$

everywhere on C. The integration of $\tilde{I}(s)$ converges rapidly using the trapezoidal rule, since $\tilde{I}(s)$ is periodic on C, and hence

$$L^{-1}(\tilde{I}(s))=\sum_{k=1}^{n}\tilde{I}(s_k)\exp(s_k t)+E_n\,, \tag{A7}$$

where

$$s_k=R\exp(i\theta_k)-R_1,\quad \theta_k=2\pi k/n\,, \tag{A8}$$

and estimates of the error E_n can be obtained from standard formulas.[16]

[1]W. E. Spear, Proc. Phys. Soc. Lond. B 76, 826 (1960); H. P. Grunwald and R. M. Blakney, Phys. Rev. 165, 1006 (1968); M. E. Scharfe, Phys. Rev. B 2, 5025 (1970); M. D. Tabak, *ibid.* 2, 2014 (1970); W. Gill, J. Appl. Phys. 43, 5033 (1972); F. B. McLean, G. A. Ausman, Jr., H. E. Boesch, Jr., and J. M. McGarity, *ibid.* 47, 1529 (1976).

[2]G. Pfister, Phys. Rev. Lett. 33, 1474 (1974); *ibid.* 36, 271 (1976); G. Pfister, S. Grammatica, and J. Mort, *ibid.* 37, 1360 (1976).

[3]J. M. Marshall and A. E. Owen, Philos. Mag. 24, 1281 (1971); J. M. Marshall and G. R. Miller, *ibid.* 27, 1151 (1973); F. D. Fisher, J. M. Marshall, and A. E. Owen, *ibid.* 33, 261 (1976).

[4]H. Scher and E. W. Montroll, Phys. Rev. B 12, 2455 (1975).

[5]J. Noolandi, following paper, Phys. Rev. B 16, 4474 (1977).

[6]F. W. Schmidlin, Solid State Commun. 22, 451 (1977).

[7]A. I. Rudenko, J. Non-Cryst. Solids 22, 215 (1976).

[8]S. K. Kim, J. Chem. Phys. 28, 1057 (1958).

[9]C. Capellos and B. H. J. Bielski, *Kinetic Systems* (Wiley-Interscience, New York, 1972).

[10]*Tables of Integral Transforms*, edited by A. Erdélyi (McGraw-Hill, New York, 1954), Vol. 2.

[11]W. D. Lakin, L. M. Marks, and J. Noolandi, Phys. Rev. B 15, 5834 (1977).

[12]R. G. Enck and G. Pfister, in *Photoconductivity and Related Phenomena*, edited by J. Mort and D. M. Pai (Elsevier, New York, 1976), p. 215.

[13]G. Pfister and H. Scher, Phys. Rev. B 15, 2067 (1977).

[14]N. F. Mott, E. A. Davis, and R. A. Street, Philos. Mag. 32, 961 (1975); P. W. Anderson, Phys. Rev. Lett. 34, 953 (1975).

[15]M. Kastner, D. Adler, and H. Fritzsche, Phys. Rev. Lett. 37, 1504 (1976).

[16]P. J. Davis and P. Rabinowitz, *Methods of Numerical Integration* (Academic, New York, 1975), p. 106.